

Investigation on parametric instabilities in laser-plasma interaction regime relevant to the generation of very strong shock waves.



INO-CNR
ISTITUTO
NAZIONALE DI
OTTICA



Gabriele Cristoforetti

*Intense Laser Irradiation Laboratory
INO-Unit "Adriano Gozzini", CNR
Pisa, Italy*

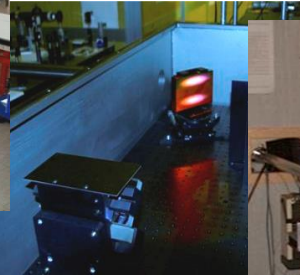
Tel. +390503152222

E-mail Gabriele.cristoforetti@cnr.it



The Intense Laser Irradiation Lab

@ INO-CNR, Istituto Nazionale di Ottica, Pisa (Italy)



PEOPLE

- Leonida A. GIZZI (CNR)* (head)
- Giancarlo BUSSOLINO (CNR)
- Gabriele CRISTOFORRETTI (CNR)
- Luca LABATE (CNR)*
- Fernando BRANDI (CNR)
- Petra KOESTER (CNR), Ric. Contr.
- Tazio LEVATO (CNR), Ric. Contr.
- Federica BAFFIGI (CNR), A.R.
- Paolo FERRARA (CNR), A. R.
- Lorenzo FULGENTINI (CNR), A.R.
- Daniele PALLA (CNR), PhD
- Antonio GIULIETTI (CNR), Assoc
- Antonella ROSSI (CNR) – Tech.



* Also at INFN

<http://ilil.ino.it>

Contributors

G. Cristoforetti, P. Koester, F. Baffigi, L. Labate, L.A. Gizzi

Intense Laser Irradiation Laboratory, INO-CNR, Pisa, Italy

Y. Maheut, G. Folpini, Ph. Nicolai, D. Batani

Université Bordeaux, CNRS, CEA, CELIA (Centre Lasers Intenses et Applications), UMR 5107, F-33405 Talence, France

F. Barbato, M. Richetta

Università di Roma "Tor Vergata," Roma, Italy

A. Marocchino, A. Schiavi, L. Antonelli, S. Atzeni

Dipartimento SBAI, Università di Roma "La Sapienza" and CNISM, Roma, Italy

J. Badziak, T. Chodukowski, Z. Kalinowska, T. Pisarczyk

Institute of Plasma Physics and Laser Microfusion, Warsaw, Poland

F. Consoli, R. De Angelis

CRE, ENEA, Frascati, Italy

E. Krousky, J. Ullschmied

Institute of Plasma Physics of the ASCR, PALS, Za Slovankou 3, 18200 Prague, Czech Republic

O. Renner, M. Smid

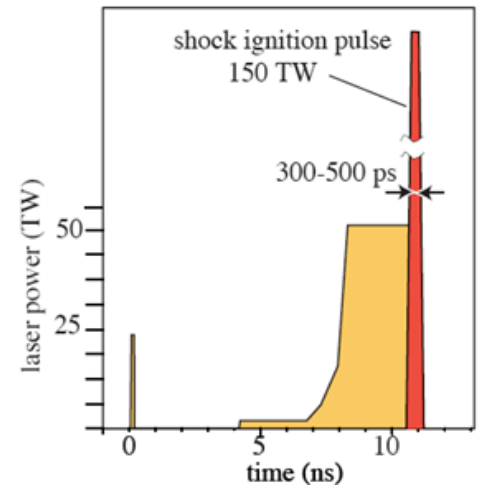
Institute of Physics of the ASCR, ELI-Beamlines/HiLASE/PALS, Na Slovance 2, 182 21 Prague, Czech Republic

M. Skoric

Vinca Institute of Nuclear Sciences, University of Belgrade, 11001 Belgrade, Serbia

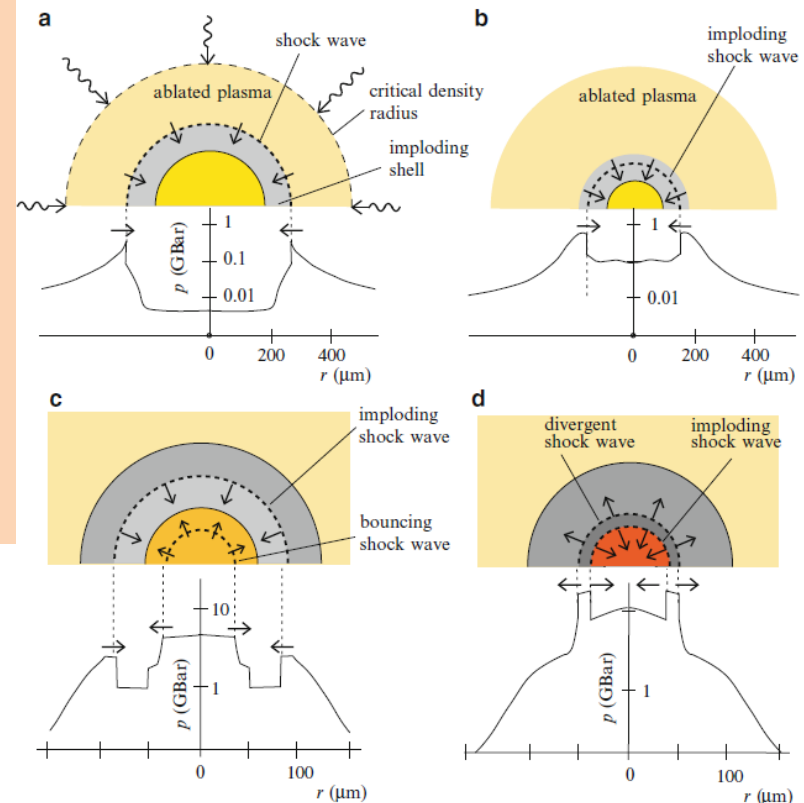
The Shock Ignition approach to ICF

- Separation of compression and ignition phase → lower implosion velocity
- Strong shock at end of compression phase to generate hot spot (intensity: 10^{15} - 10^{16} W/cm²)
- Geometrical amplification of spherically converging shock (ablation pressure 200-300 Mbar)



Advantages vs. standard ICF and fast ignition

- Lower implosion velocity (250 km/s vs. 350-400 km/s) → lower Rayleigh Taylor Instability, higher energy gain (50-100)
- Scheme robust: target displacement up to 15 μ m, tolerance to nonuniform spike irradiation, non critical synchronization of the ignition pulse (150-250 ps)
- A single laser can be used for compression and ignition
- Lasers needed for shock ignition are already available (LMJ, NIF)



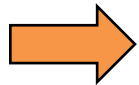
X. Ribeyre et al., PPCF 51, 015013 (2009)

R. Betti et al., PRL 98, 155001 (2007)

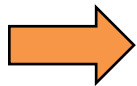
S. Atzeni, PPCF 51, 124029 (2009)

Shock Ignition – Open Issues

Laser-Plasma Interaction regime of ignition pulse (10^{15} - 10^{16} W/cm²) is dominated by parametric instabilities - **Stimulated Brillouin Scattering (SBS)**, **Stimulated Raman Scattering (SRS)** and **Two Plasmon Decay (TPD)** – and filamentation



a significant **backscattered energy** can increase laser energy requirements.



generation of **fast electrons** (SRS, TPD)

Expected energy < 100 keV → stopped in the high- ρ R shell ($\gg 17$ g/cm²) of the pre-compressed capsule at end of compression.

Simulations including fast electrons show no gain degradation and larger time window.

L.J. Perkins et al., PRL 103, 045004 (2009)., R. Betti et al., J.Phys.:Conf.Ser. 112, 022024 (2008)

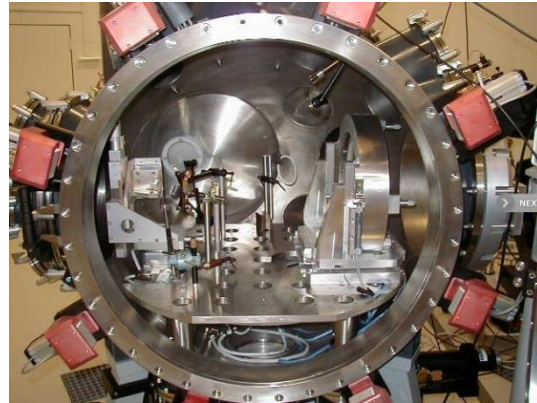


They can have a **beneficial effect on pressure**

Nora et al. Phys. Rev. Lett. 114, 045001 (2015)

(Effects of non-local heat transport must be investigated but it might also be beneficial,

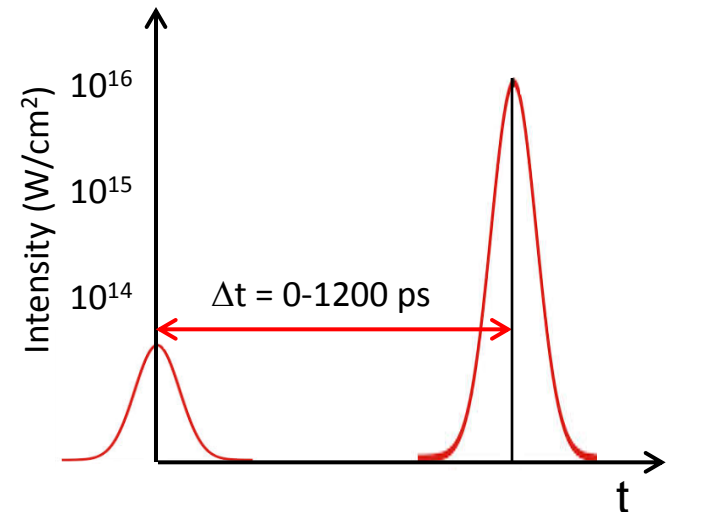
A.R. Bell and M. Tzoufras, PPCF 53, 045010 (2011))



1ω $\lambda=1.315 \mu\text{m}$, $t \approx 250 \text{ ps}$ $E = 1000 \text{ J}$
 3ω $\lambda=438 \mu\text{m}$, $t \approx 250 \text{ ps}$, $E_{\text{max}} = 300 \text{ J}$
 $f/2$ focussing lens

Objectives

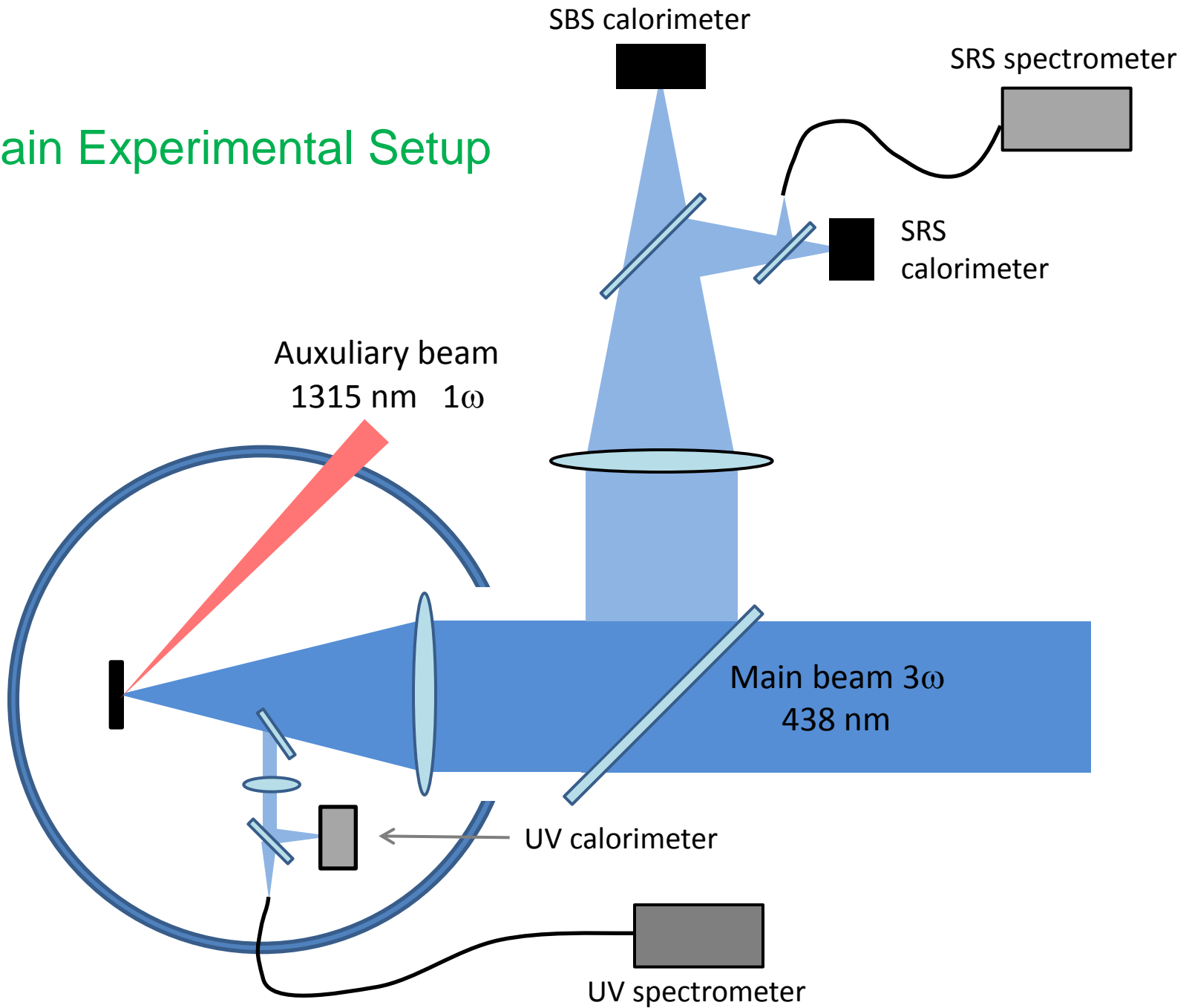
- Assessing the importance of parametric instabilities
- Characterization of fast electrons
- Determination of shock pressure
- Assessing the dependence on preplasma scalelength



Pre pulse 1ω
 $7 \cdot 10^{13} \text{ W/cm}^2$
 Produces a
 preplasma

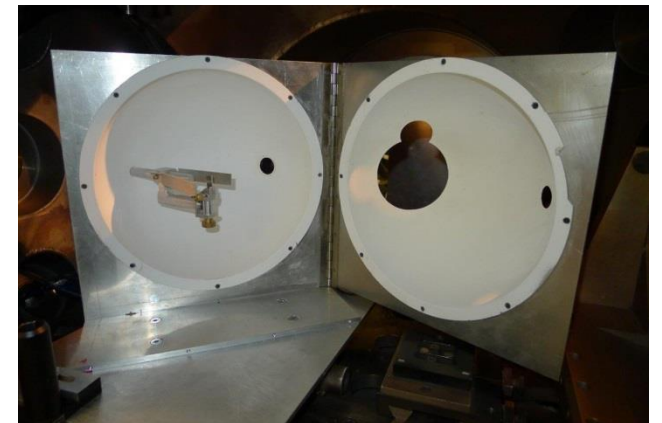
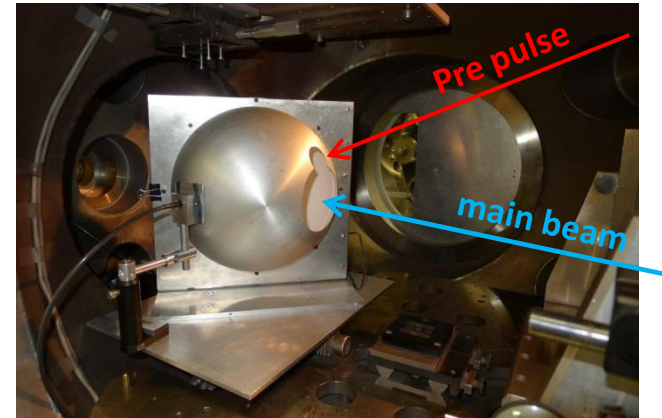
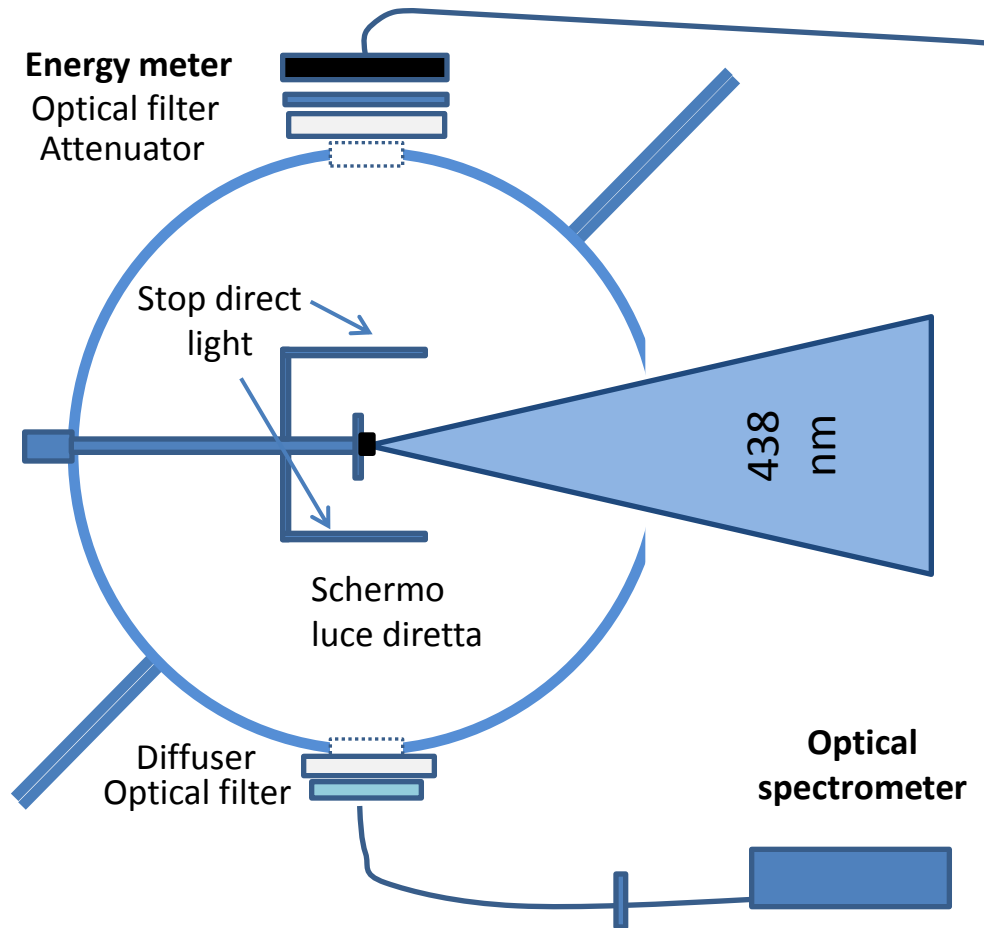
Ignitor pulse 1ω or 3ω
 $10^{15} - 10^{16} \text{ W/cm}^2$
 Launches the shock

Main Experimental Setup



Experimental setup 2

Aim: quantifying the visible radiation reflected outside the lens cone (SBS, SRS, TPD, laser)

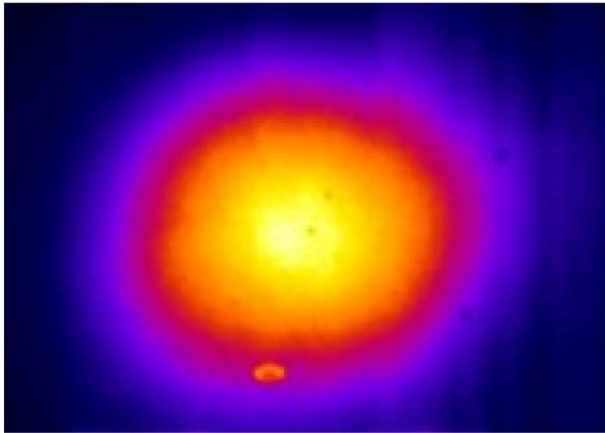


The role of filamentation

Pre pulse spot = 900 μm
(1D plasma)

Random Phase Plate (RPP)

Gaussian FWHM = 100 μm



no evident hot spots

Spatial coherence

the random pattern of phase shifters along the laser path results in the reduction of spatial coherence length

$$\lambda_{\perp} \approx 2F\lambda_0$$

$$\lambda_{\parallel} \approx 8F^2\lambda_0$$

Speckles $\approx 1.6 \mu\text{m} \times 1.6 \mu\text{m} \times 14 \mu\text{m}$

Intensity distribution in speckles

$$u = I_{sp} / \langle I \rangle$$

$$f(u) \propto u e^{-u}$$

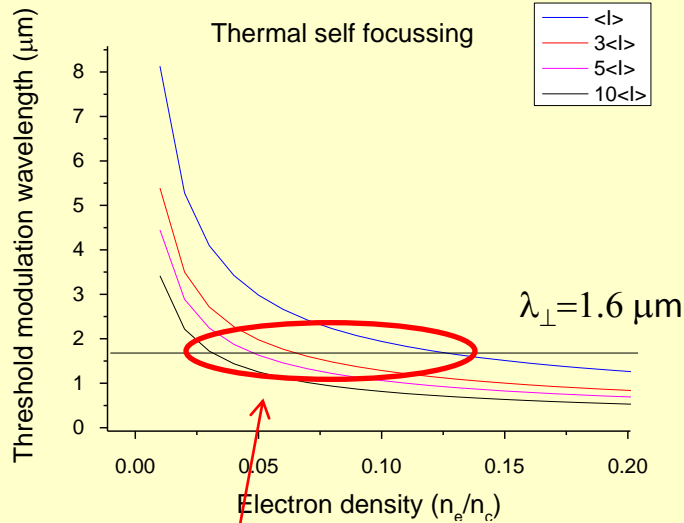
$$\langle I \rangle = (3-9) \cdot 10^{15} \text{ W cm}^{-2}$$

High-energy tail up to 5-10 $\langle I \rangle$

$$5\langle I \rangle = (4.5) \cdot 10^{16} \text{ W cm}^{-2}$$

$$10\langle I \rangle = 9 \cdot 10^{16} \text{ W cm}^{-2}$$

Smallest perturbation length λ_{\perp} able to drive thermal filamentation



- thermal filamentation prevails at early times while ponderomotive filamentation is dominant near the peak of the laser pulse
- filamentation is expected to occur at densities larger than $n_e \sim 0.05 n_c$
- Filamentation is expected to occur at early times

Thermal spatial growth rate

$$k_{\perp} = 2\pi / \lambda_{\perp}$$

$$k_g = \frac{\omega_0}{2c\sqrt{\epsilon}} \left\{ 2 \frac{n_e}{n_c} \gamma_T \left[1 + (30k_{\perp}\lambda_e)^{4/3} \right] - \frac{k_{\perp}^4}{k_0^4} \right\}^{1/2}$$

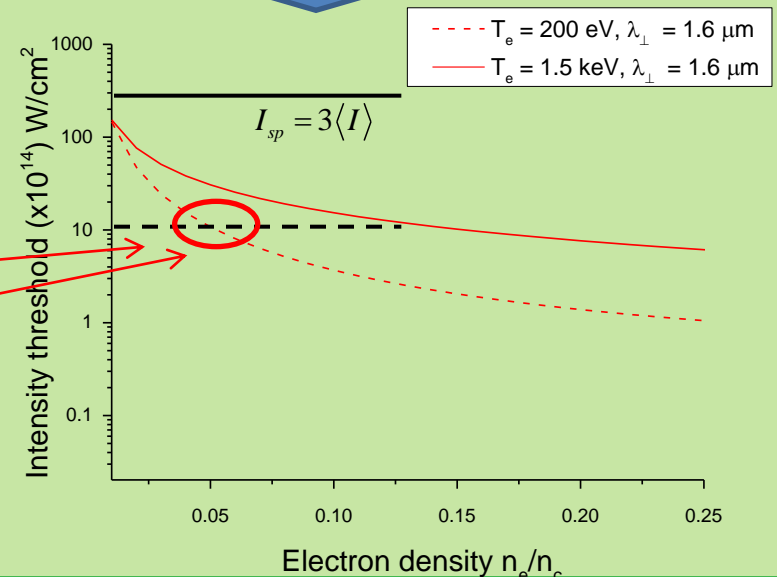
non local electron heat transport effects

$$k_{\perp}\lambda_e > 0.1$$

γ_T is the ratio between inverse bremsstrahlung and thermal conduction rates given by Spitzer-Harm conductivity

$$k_g L_{SP} = 1$$

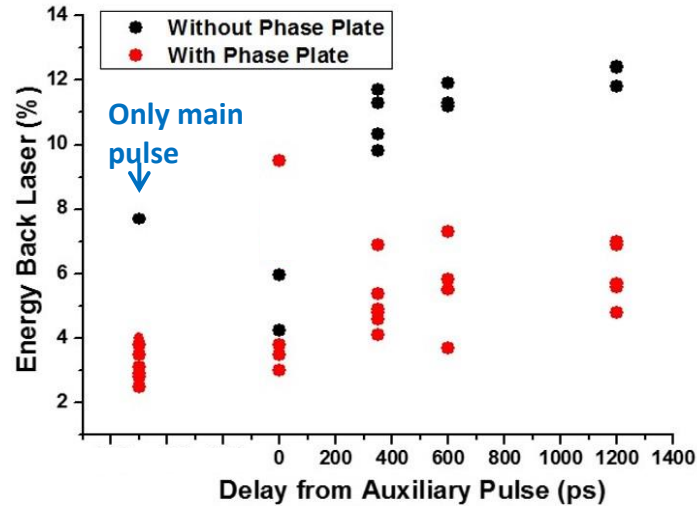
$$L_{SP} = 14 \mu\text{m}$$



Stimulated Brillouin Scattering and backreflected laser

Backscattered energy into the lens cone vs. delay

$$\omega_S \approx \omega_0$$

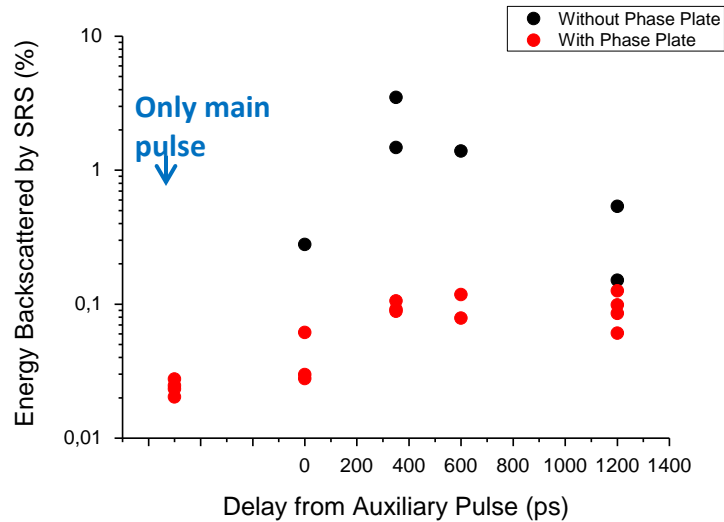


- Backscattered energy in the lens cone is **2-7%** of laser energy.
- Scattered energy in all the solid angle (integrating sphere) is **> 17-23%**.
- Dominant contribution from backreflected laser and SBS, in agreement with similar experiments*.
- Signal increases with increasing preplasma extension.

* C. Goyon et al., Phys. Rev. Lett. 111, 235006 (2013).
S. Depierreux, Phys. Plasmas **19**, 012705 (2012).

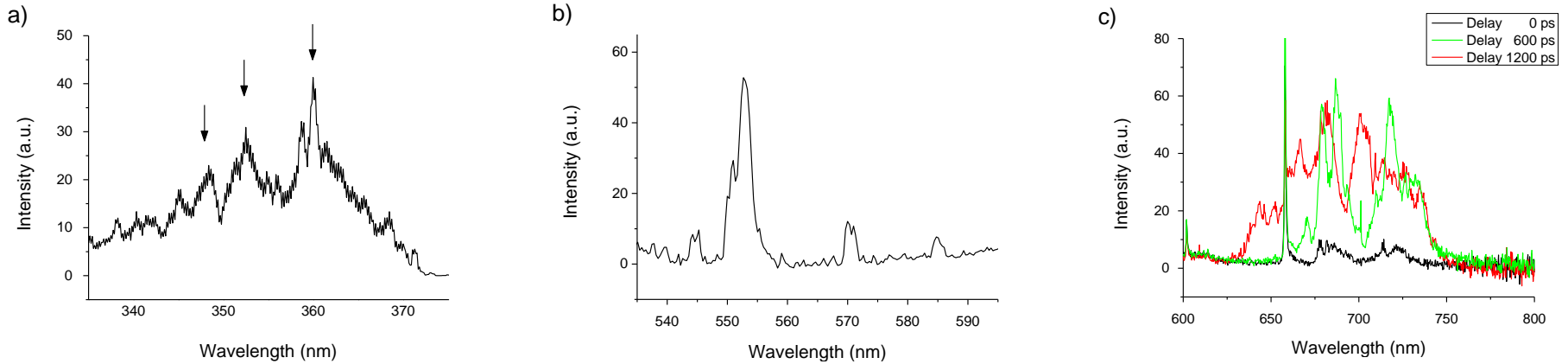
Stimulated Raman Scattering ($n_e < n_c/4$)

$$\omega_0 < \omega_S < 2\omega_0$$



- Energy backscattered by SRS is $< 0.12\%$ of laser energy (not relevant for energy dissipation).
- Signal increases with increasing preplasma extension.

Stimulated Raman Scattering



SRS threshold due to inhomogeneity mismatch and Landau damping

Inhomogeneity $\rightarrow \kappa = k_0 - k_s - k_e$

$$\int_0^l \kappa dx \approx 1/2$$

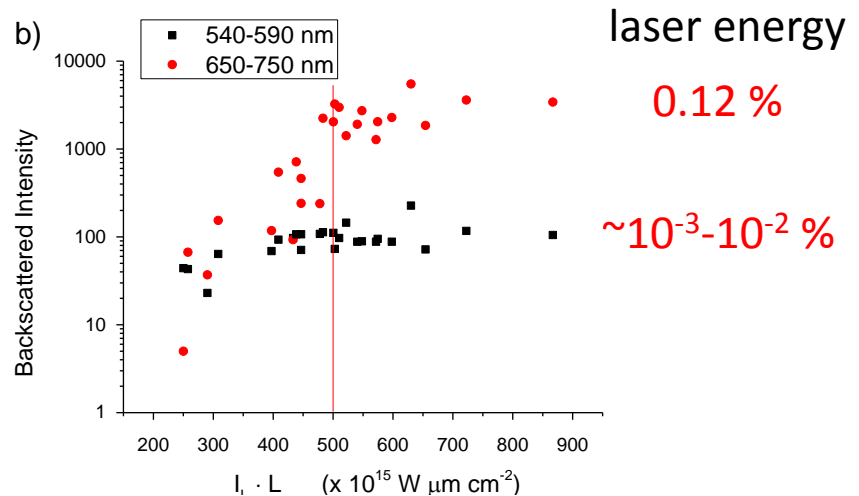
Exponential profile $\exp(-z/L)$ can be considered linear since $l \approx 2 \mu\text{m}$ and $l \ll L$

For linear mismatch $\kappa(x) = \kappa'x$

Standard convective theory

$$I_{SRS} = \exp(\pi\lambda)$$

$$\lambda = \gamma_0^2 / \kappa' |v_e v_s| \propto I \cdot L$$



Backward SRS

$$0.1 < n_e/n_c < 0.16$$

Absolute vs. Convective SRS discussion

$\lambda \gg 1$ \rightarrow Absolute SRS can occur

$$\frac{v_0^2}{c^2} > 4|k_e - k_0| / k_e^2 L \quad \text{BRS threshold}$$

$$I^{BRS} = (4-8) \cdot 10^{15} \quad I_L \cdot L = 500$$

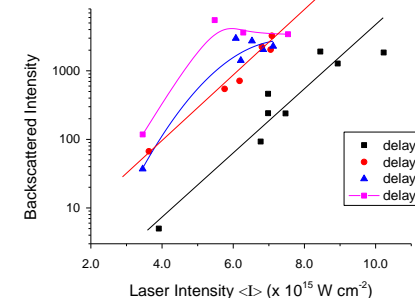
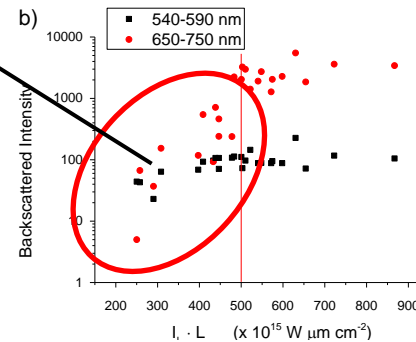
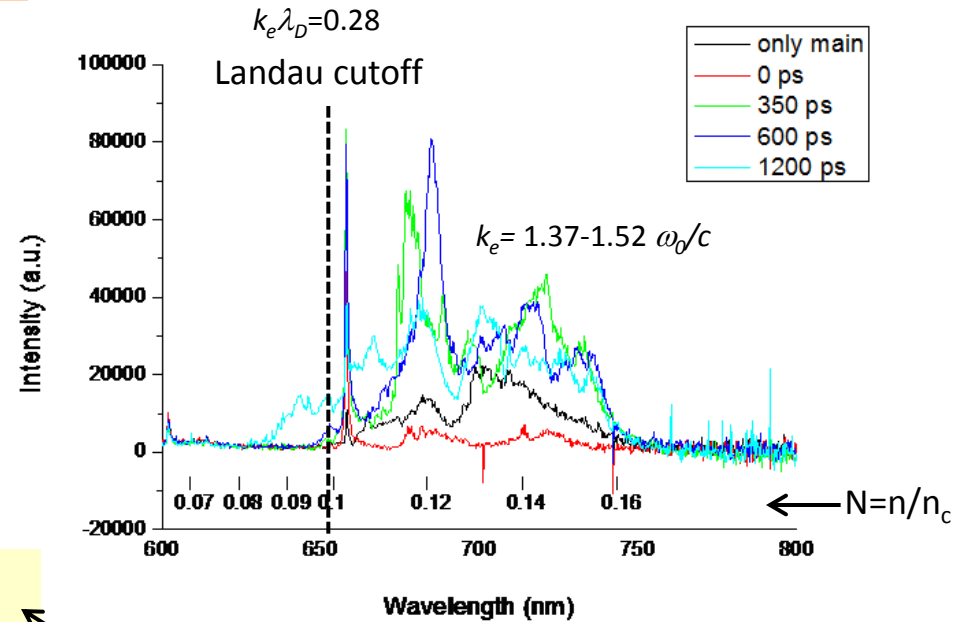
1 - SRS growth at $\langle I \rangle < I^{BRS}$ can be due to the overcome of the threshold in speckles

2 - We observe a rapid growth 1-2 orders of magnitude in a factor 2 laser intensity and then a rapid saturation.

In agreement with simulations accounting for kinetic effects ($k_e \lambda_D > 0.15$) and with experiments at Trident laser facility aimed at investigating SRS occurring in single hot spots.

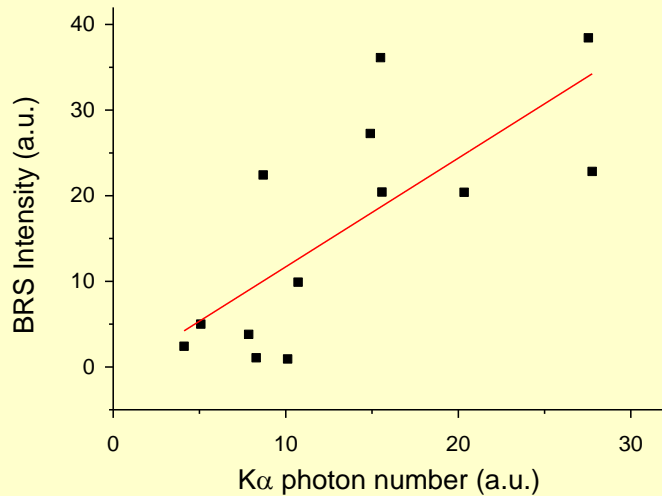
3 - Saturation can be due to nonlinear frequency detuning produced by bowing and filamentation of plasma waves in speckles; LDI, electron trapping in nonlinear

4 - Intensity dependent spectral broadening is attributed to nonlinear saturation of BRS with large bursts and quasi-periodic pulsations in intensity (not necessarily different densities)



Backward SRS and hot electrons

1 – Correlation between Raman signal and $K\alpha$ photon number



Hot electron temperature calculated from stopping power and Ti/Cu layers

$$T_{\text{hot}} = 28 \text{ keV} \pm 4 \text{ keV}$$

$$\nu_{\text{hot}} = \nu_{\text{ph}}^{\text{EPW}}$$

Hot electron energy expected from BRS at $0.1\text{-}0.15 n_c$

$$T_{\text{hot}} = 20 \text{ keV} \pm 3 \text{ keV}$$

Hot electron energy expected from TPD

$$k_e = 3k_0$$

$$T_{\text{hot}} = 10 \text{ keV}$$

$$k_e = k_0$$

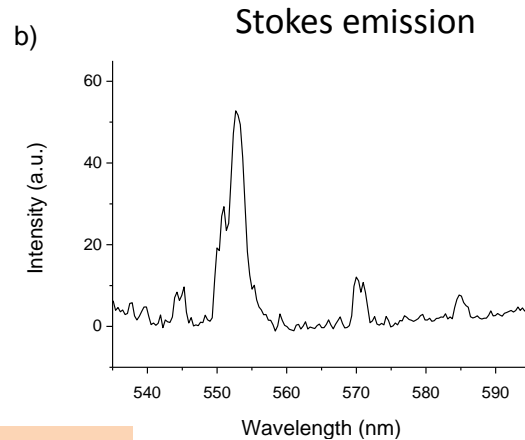
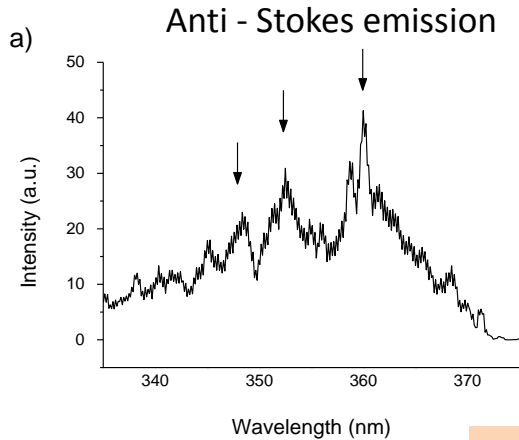
$$T_{\text{hot}} = 114 \text{ keV}$$

2 – Experimental hot electron temperature agrees with energy expected from SRS EPW breaking.



fast electron generation is mainly due to SRS

Forward SRS



$$n_e/n_c \approx 0.04$$

threshold

$$\left(\frac{\nu_{osc}}{c}\right)^2 > \frac{4}{k_0 L} \left(\frac{\omega_0}{\omega_p}\right)^3$$

$$I^{FRS} = (3-6) \cdot 10^{17} \quad I_L \cdot L = 30000$$

- It is difficult to associate these peaks to BRS $k_e \lambda_D = 1$, unless it occurs in inflationary regime
- We observe AntiStokes peaks at intensities comparable to Stokes peaks

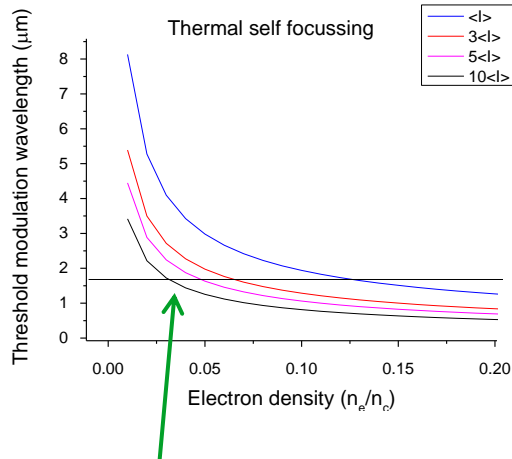


Forward Raman Scattering

But how we can we see it ?

- Reflection at n_c ?
- SBS of FRS bursts*
SBS threshold in the range $10^{14}-10^{15} \text{ W cm}^{-2}$

Forward SRS and filamentation



Filamentation into speckles

-> modify density profile, saddles, local maximums, ecc.

-> Local increase of laser intensity

We expect filamentation at $n_e = 0.05-0.07 n_c$

In steady state filaments

$$n_0 = N_0 e^{-v_0^2/4v_e^2} \quad \frac{v_0}{v_e} \cong \sqrt{2}/2$$

$$\varepsilon = \frac{N - n_0}{N} \approx 0.12$$

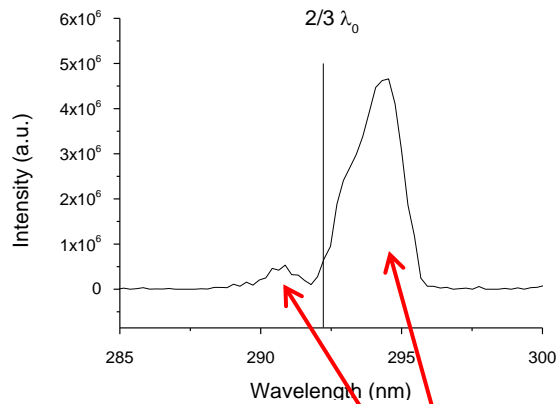
Depletion at the bottom of the filament

Real expected $\varepsilon = 0.1-0.2$

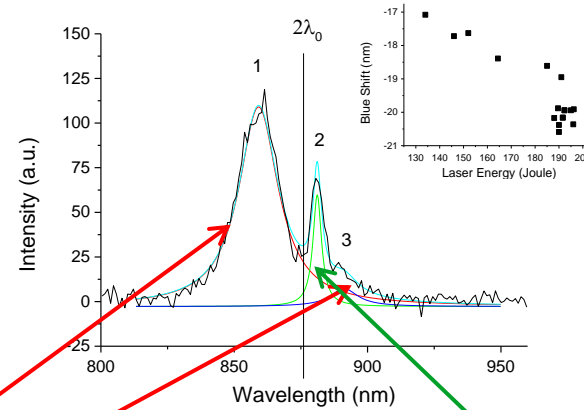
Therefore, intense speckles $I_{sp} > 5\langle I \rangle = 5 \cdot 10^{16} \text{ W cm}^{-2}$ undergo filamentation at $n_e = 0.05-0.07 n_c$, FRS occurs at the bottom of filaments where $n \approx 0.04 n_{cr}$

Half-harmonics: $3/2\omega_0$ and $\omega_0/2$

$n_e/n_c \approx 0.25$



TPD



Hybrid TPD/SRS

TPD: a laser photon decays into 2 EPWs

Energy gap between plasma waves

$$\Delta\omega/\omega_0 = \frac{9}{4} \left(v_e^2 / c^2 \right) \kappa$$

$$\kappa = \mathbf{k}_B \cdot \mathbf{k}_0 / k_0^2 - 1/2$$

$\omega_0 - \omega_p$
 $\omega_p \rightarrow \omega_s$ or



$$\kappa \approx 2 \rightarrow k_e \approx 3k_0$$

$$k_e \lambda_D \approx 0.3$$

near the Landau cutoff



$$\kappa = 1/2 \rightarrow k_e \approx k_0$$

$$\Delta\lambda_{therm} = \frac{9}{2} \frac{T(\text{keV})}{511} \lambda_L$$

$$T_e \approx 1.5 \text{ keV}$$

Considerations on energy dissipated at $n_c/4$

- **Laser photons reach $n_c/4$ surface** but half-harmonics generation efficiency is very low ($\eta_{1/2} \approx 10^{-3} \%$, $\eta_{3/2} \approx 10^{-1} \%$)
- **Non relevant degradation of laser-plasma coupling**; it is however plausible, that such efficiency could be much higher at early times, when TPD is expected to prevail on other instabilities.
- **Absolute SRS occurring at $n_c/4$ is here replaced by a hybrid TPD/SRS instability** giving rise to a blue plasmon with $k \approx k_0$, which is contrast with large-scale kinetic simulation of laser-plasma interaction in SI conditions⁺. Some simulations, however, refer to plasma temperatures of 5 keV, which result in a strong Landau damping of SRS at $n_e < n_c/4$. These simulations are either 1D simulations, overestimating SRS extent, or they are 2D simulations but limited to a few picoseconds time. TPD seems to prevail according to Weber et al.*

⁺ O. Klimo, V.T Tikhonchuk, Plasma Phys. Control. Fusion 55 (2013) 095002; O. Klimo, J. Psikal, V. T. Tikhonchuk, S. Weber, Plasma Phys. Control. Fusion **56** (2014) 055010.

* S. Weber, C. Riconda, High Power Laser Science and Engineering, 3, e6 doi:10.1017/hpl.2014.50, (2015).

Conclusions

- The energy backscattered in the lens cone is 2-7% and **dominated by laser/Stimulated Brillouin Scattering**, slightly increasing with plasma scalelength. **Overall scattered light is >20%**.
- **Energy backscattered by SRS is limited to 0.03-0.12%, dominated by BRS** occurring in the density region 0.10-0.15 n_c , near the Landau cutoff.
- **Two Plasmon Decay instability prevails on absolute SRS at $n_c/4$ density**. The odd-harmonics generation efficiency - $\eta_{1/2} \sim 10^{-3}$ %, $\eta_{3/2} \sim 10^{-1}$ % - gives rise to an irrelevant loss of laser energy. There is a striking difference with numerical simulations in SI conditions, all resulting in a relevant fraction of energy scattered by the absolute SRS in this density region.
- RPP results in a strong suppression of FRS and in a weak reduction of BRS (~a factor 2). This effect is produced by the large fraction of laser energy in high-intensity hot spots in shots w/o RPP, which is much higher than the fraction of energy included in high-intensity speckles when RPP is used.
- The impact of **small-scale filamentation is a determining factor** in laser-corona interaction. The occurrence of filamentation is suggested by 1) the overcome of FRS threshold, 2) the strong increase of FRS in shots without RPP, 3) the density regions where filaments are expected to form, 4) the modulation of FRS light spectra, which are compatible with eigenfunctions of EPW energy into the filaments.
- Experimental results suggest that **hot electrons are generated by the breaking of BRS plasma waves**.
- RPP shots with higher energy and longer delay show **evident signs of BRS saturation**. This agrees with the complex profile of BRS light spectra, explained by frequency detuning in strong EPW, due to ponderomotive or electron trapping as for example in bowing and filamentation of plasma waves. **Saturation could limit BRS extent at longer density scalelength, which becomes essential in real SI conditions, but the effect of temperature could be very important (to be investigated)**.

THANK YOU FOR YOUR ATTENTION !

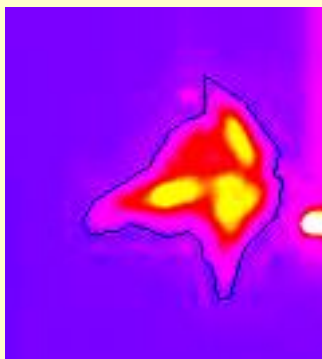
References:

- D. Batani et al, J. Phys.: Conf. Ser. 399, 012005, 2012
- P. Koester et al., Plasma Phys. Control. Fusion 55, 124045, 2013
- D. Batani et al., Phys. Plasmas 21, 032710, 2014
- T. Pisarczyk et al., Phys. Plasmas, 21, 012708, 2014
- Y. Maheut et al., Physica Scripta 2014 (T161), 014017
- J. Badziak et al., Laser and Particle Beams 33, 161, 2015
- G. Cristoforetti, submitted to Nuclear Fusion

The role of filamentation: focal spot

Original beam

Diameter 60 μm



2-3 hot spots

$$\lambda_{\perp} = 15-20 \mu\text{m}$$

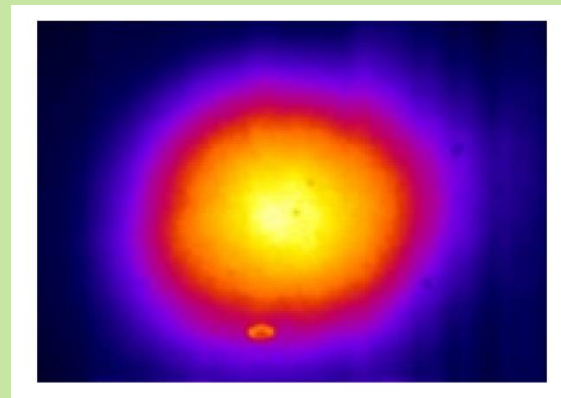
$$\langle I \rangle = (1-2) \cdot 10^{16} \text{ W cm}^{-2}$$

More than 50% energy enclosed in hot spots

$$\langle I \rangle = (3-4) \cdot 10^{16} \text{ W cm}^{-2}$$

Random Phase Plate (RPP)

Gaussian FWHM = 100 μm



no evident hot spots

$$\lambda_{\perp} \approx 2F\lambda_0$$

$$\lambda_{\parallel} \approx 8F^2\lambda_0$$

Speckles $\approx 1.6 \mu\text{m} \times 1.6 \mu\text{m} \times 14 \mu\text{m}$

$$u = I_{sp} / \langle I \rangle$$

$$f(u) \propto ue^{-u}$$

$$\langle I \rangle = (3-9) \cdot 10^{15} \text{ W cm}^{-2}$$

High-energy tail up to 5-10 $\langle I \rangle$

$$5\langle I \rangle = (4.5) \cdot 10^{16} \text{ W cm}^{-2}$$

$$10\langle I \rangle = 9 \cdot 10^{16} \text{ W cm}^{-2}$$

Original beam

Thermal growth rate

$$k_g = \frac{\omega_0}{2c\sqrt{\epsilon}} \left\{ 2 \frac{n_e}{n_c} \gamma_T \left[1 + (30k_{\perp}\lambda_e)^{4/3} \right] - \frac{k_{\perp}^4}{k_0^4} \right\}^{1/2}$$

$$k_{\perp} = 2\pi / \lambda_{\perp}$$

non local electron heat transport effects $k_{\perp}\lambda_e > 0.1$

γ_T is the ratio between inverse bremsstrahlung rate and thermal conduction rate given by Spitzer-Harm conductivity

$$k_g L = 1$$

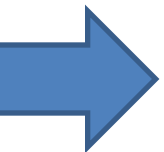
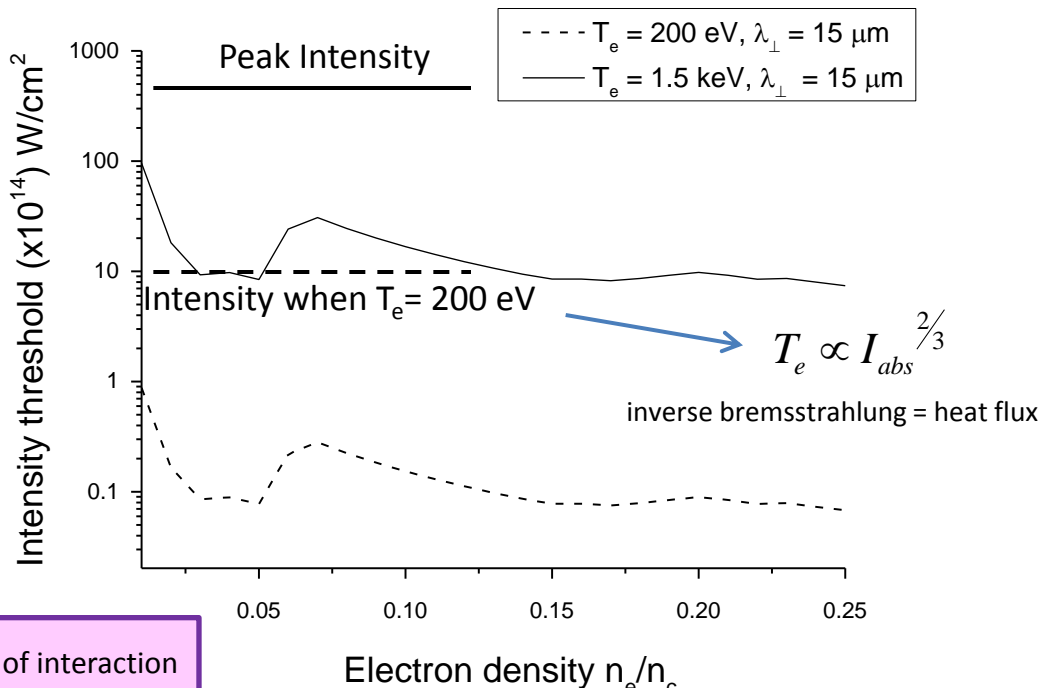


$$L = n / (dn/dx)$$

from hydrodynamic simulations

L = 35-70 μm preplasma

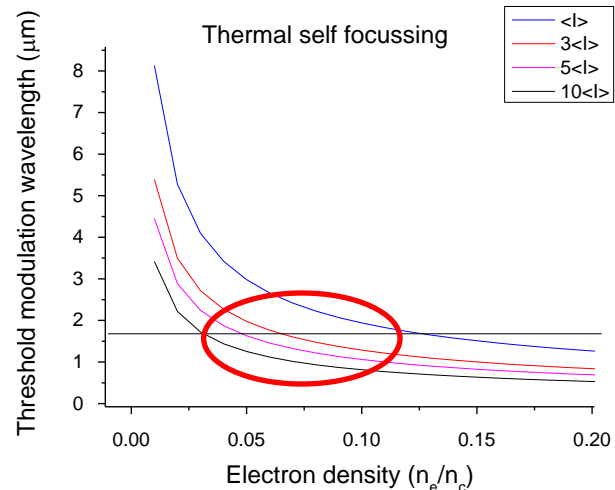
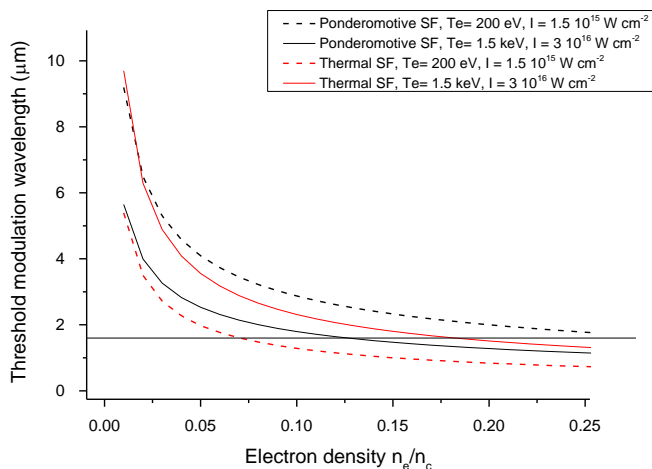
L = 50-100 μm main pulse



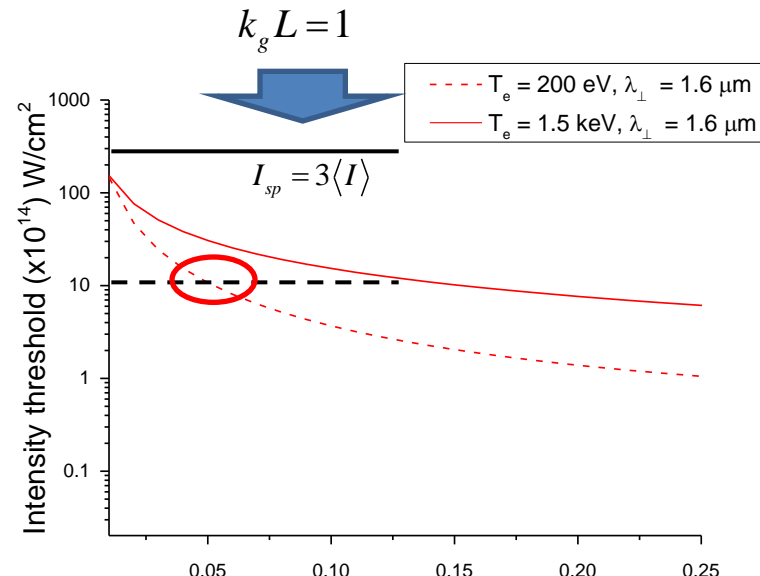
- Self-focusing of hot spots occurs at early times of interaction and at low densities, modifying the following propagation of the laser beam.
- Filaments successively could break in smaller radius filaments, of the order of 3-6 μm , (optimal modulation wavelengths)

Random Phase Plate

$$I_{sp} = 3\langle I \rangle = 3 \cdot 10^{16} \text{ W cm}^{-2}$$



- thermal filamentation prevails at early times (dashed lines) while ponderomotive filamentation is dominant near the peak of the laser pulse (solid lines)
- filamentation does not occur for densities lower than $n_e \sim 0.07 n_c$
- Filamentation is expected to occur at early times

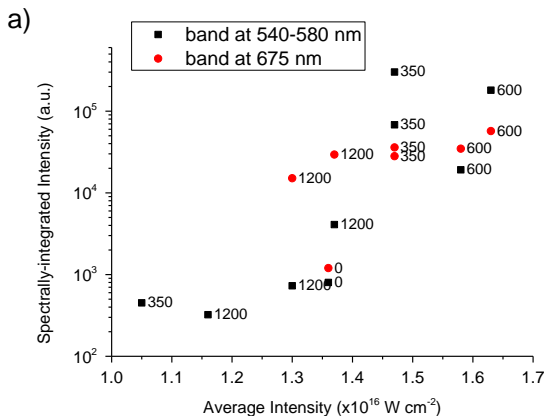
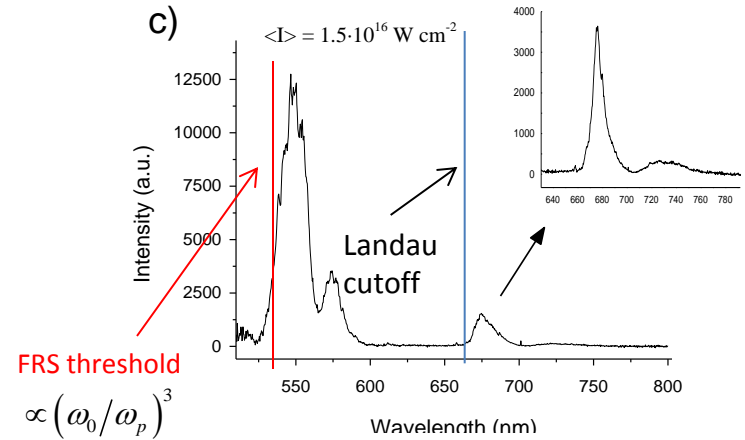
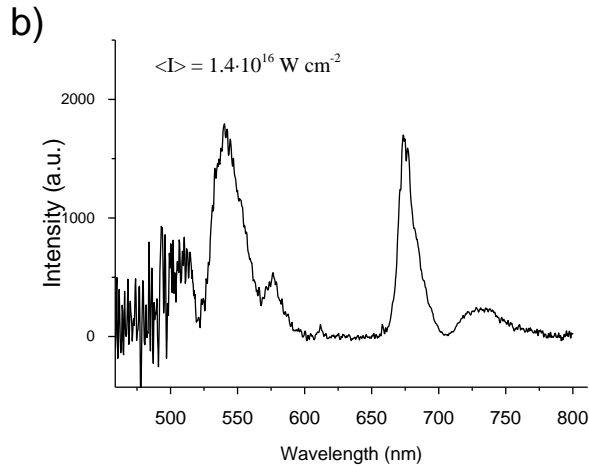


Shots w/o RPP

$$\langle I \rangle \approx (1-2) \cdot 10^{16} \text{ W cm}^{-2}$$

More than 50% energy at $I_{\text{hot spots}} \approx (3-4) \cdot 10^{16} \text{ W cm}^{-2}$

- Laser/SBS backscatter = 6-12% of the laser energy
- Energy backreflected by SRS = 0.3-3% of the laser energy, most of which (~90%) from $n_e \approx 0.04-0.06 n_c$



FRS grows very rapidly

BRS saturates

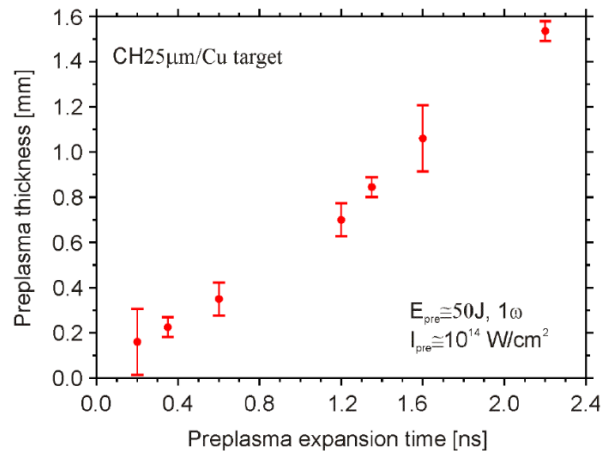
(According to theory)

Frequency modulation could be due to self focussing of the 2-3 large hot spots in the beam

Preplasma characterization

- Preplasma density through optical 3-frame interferometry

Preplasma size at density 10^{19} cm^{-3}



- Plasma expands linearly in time
- At largest experimental delay (1200ps) plasma dimension (at 10^{19} cm^{-3}) is 0.7mm.

- From hydrodynamic simulations, the preplasma scalelength at density $0.05 < n_c < 0.2$, typical of SRS instability the density scalelength is in the range 30-70 μm
- Preplasma temperature through high resolution X-ray spectroscopy

Preplasma temperature $\sim 175 \text{ eV}$ (time-integrated)

$3/2\omega_0$ emission

Considering maximum growth rate of TPD and plasmon propagation required for the coupling

$$k_y = 3\omega_0 \sin \theta / 2c$$



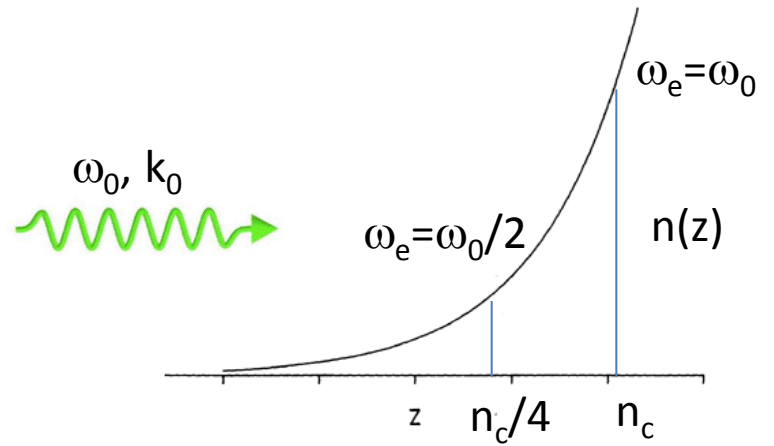
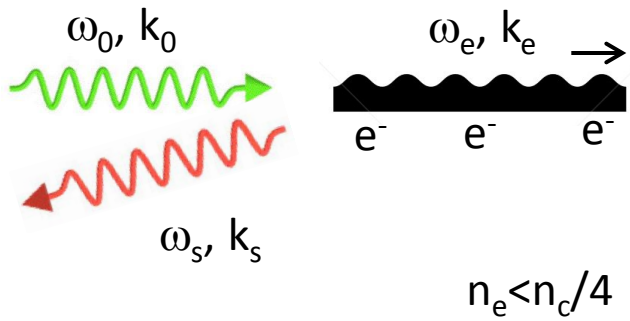
$$T_e = 1.7-3.3 \text{ keV} \quad \text{depending on laser intensity}$$

In agreement with hydrodynamic simulations but other diagnostics lead to temperature of 1.5-2 keV

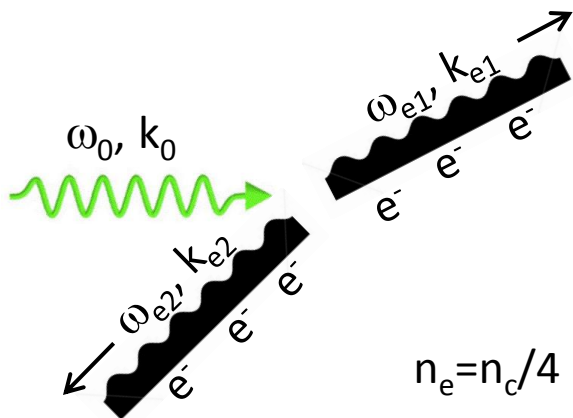
It is known that $3/2\omega_0$ emission is not suitable for temperature diagnostics because it is affected by geometry of interaction and 2D effects (filamentation, turbulence, cavitation). Usually it overestimates the temperature

For example, by using the approach of Short et al.* of $3/2\omega_0$ formation in filaments we estimate a lower plasma temperature of $\sim 1.1-1.5$ keV

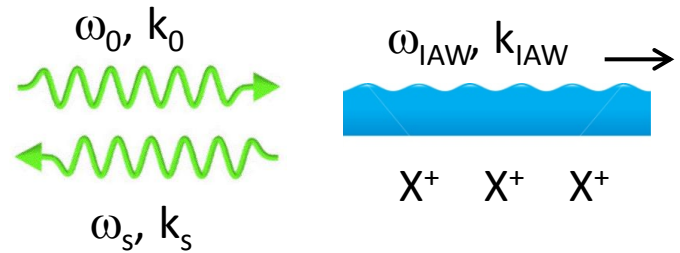
Stimulated Raman Scattering



Two Plasmon Decay

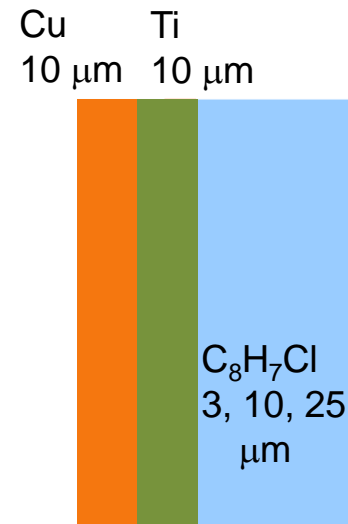
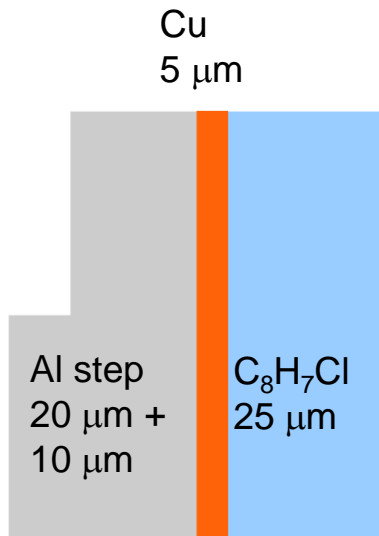


Stimulated Brillouin Scattering

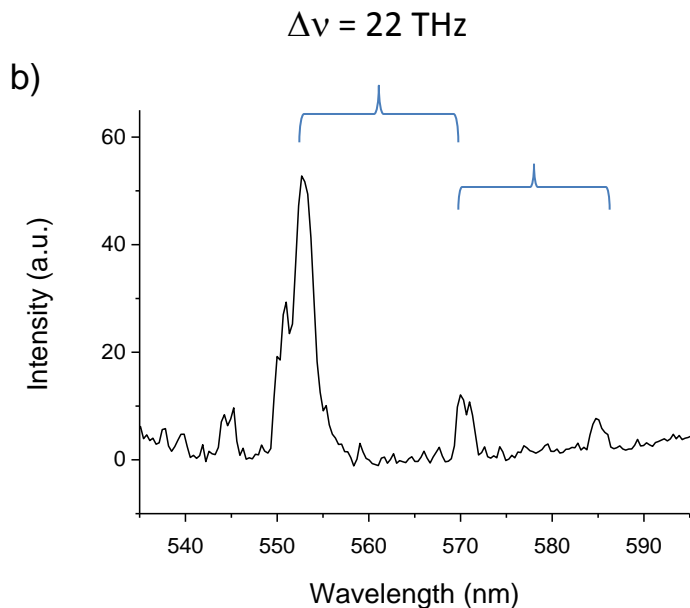


Targets

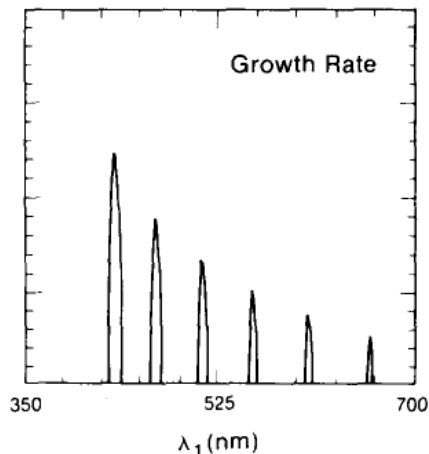
- Plastic layer to simulate capsule ablator material
- Cl in plastic to perform temperature measurements (X-ray spectroscopy)
- Cu and Ti layers for fast electron detection ($K\alpha$ measurements)
- Al layer for shock chronometry (EOS of Al is well known)



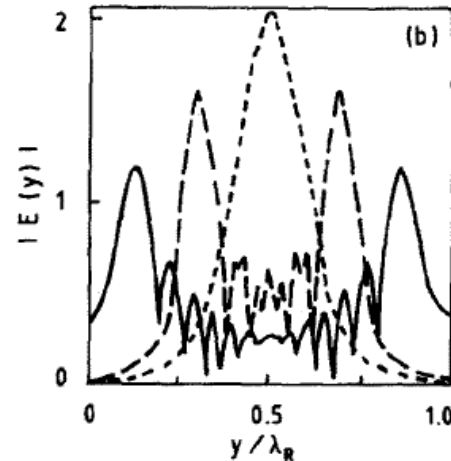
Modulation of Forward SRS



R.W. Short et al., Phys. Fluids 30, 3245, 1987



H.C. Barr et al., Phys. Fluids 31, 641, 1988.



Plasma waves propagate in a filament as in a waveguide in **discrete bound modes**, corresponding to the eigenfunctions of the Schroedinger equation describing radial distribution in the potential well

$$\Delta\omega_{mod} = (6\varepsilon)^{1/2} \frac{\pi}{2a} v_e$$

a is the filament radius

$$\varepsilon = 0.15$$

$$a \approx c/\omega_p \quad \text{skin depth}$$



$$\Delta\lambda_{exp} = 22 \text{ nm}$$

It supports our hypothesis !